Fruit Research

ARTICLE

Open Access

https://doi.org/10.48130/frures-0024-0024

Fruit Research **2024**, 4: e030

Genome-wide identification and characterization of MdCYP86A family in apple

Hui-Min Lv[1], Rui-Han Qi[1], Zi-Han Yu[1], Yao-Yang Man[1], Yan-Hui Lv[1], Han Jiang[1], Tao Wang[2], Ya-Li Zhang[1*] and Yuan-Yuan Li[1*]

[1] *National Apple Engineering Technology Research Center, Shandong Collaborative Innovation, Center of Fruit & Vegetable Quality and Efficient Production, College of Horticulture Science and Engineering, Shandong Agricultural University, Tai-An 271018, Shandong, China*

[2] *Tai' an Institute For Food And Drug Control, Tai-An 271000, Shandong, China*

* Corresponding authors, E-mail: ylzhang0522@163.com; liyy0912@163.com

Abstract

The cytochrome P450 enzyme is one of the largest protein families identified in cuticle biosynthesis, plant growth, development, and stress response. In the present study, 28 members of the MdCYP86A family were identified in apple (*Malus* × *domestica* Borkh.). Chromosomal localization analysis found that 28 genes were distributed on 13 chromosomes in apple. Phylogenetic and conserved motifs analysis showed that MdCYP86As in apple is evolutionarily most closely related to *Arabidopsis thaliana*. Each gene contains a cytochrome P450 domain, suggesting that MdCYP86As are highly conserved during the evolution of the species. Cis-acting element analysis of the promoter identified various elements associated with stress response. *MdCYP86A21* was cloned in the apple genome to investigate the function of MdCYP86A family genes. *MdCYP86A21* responded to abiotic stress, including PEG, NaCl, and ABA. The tissue-specific expression patterns revealed that the highest expression tissue was in flower by real-time quantitative reverse transcription (RT-qPCR). Subcellular localization showed that MdCYP86A21 was localized in the endoplasmic reticulum. Further, the function of *MdCYP86A21* to enhance the resistance to PEG and NaCl stress in apple calli was verified. These results contribute to further study on the function of MdCYP86As and provide a molecular basis for the study of apple stress tolerance.

Citation: Lv HM, Qi RH, Yu ZH, Man YY, Lv YH, et al. 2024. Genome-wide identification and characterization of MdCYP86A family in apple. *Fruit Research* 4: e030 https://doi.org/10.48130/frures-0024-0024

Introduction

The plant cuticle is a natural barrier in plants to adapt to the external environment, and the role of the cuticle is to effectively improve drought stress, reduce ultraviolet radiation, prevent the attack of pests and diseases, reduce non-stomatal water loss, and block organ fusion[1–4]. The cuticle consists of cutin and cuticular wax. The main components of cutin were C16 and C18 fatty acid and cuticular wax were very-long-chain fatty acids and their derivatives consist of alkane, alcohol, aldehyde, ester, and so on[5,6]. Wax is soluble in organic solvents and its crystal structure is observed using modern microscopic techniques[7]. The crystal structure of cuticular wax varies in different species, mainly in spherical, lamellar, rod-like, and so on[2,7–9].

In the process of wax biosynthesis, C16, and C18 fatty acids are synthesized in plastids, followed by the extension of short-chain fatty acids into C26–C34 very-long-chain fatty acids and their derivatives by the action of long-chain acyl CoA synthase (LACS)[10–12]. The generated very long chain fatty acids (VLCFA) are extended into acyl-coenzyme A, which in turn forms primary alcohols and wax esters *via* the acyl reduction pathway. In the alkane formation pathway, aldehyde is formed first, followed by decarbonization to produce alkane, and finally the transition from alkane to secondary alcohol and ketone is achieved by a two-step redox reaction[13,14]. In the process of wax biosynthesis, we identified the involvement of *MdCYP86A21* in the successive two-step oxidation reaction to achieve the transformation from alkane to alcohol in apple[14]. The wax monomers formed are transported to the plasma membrane *via* ABC and LTP transporter proteins, which in turn, form wax to cover the plant surface[7,15].

Cytochrome P450 is one of the largest enzyme families in plants, named because of the special absorption peak at 450 nm and this family of proteins plays an important role in plant metabolism and development and adaptation to the environment[16–19]. The gene functions of the CYPs family are involved in signal transduction, biological stress, polymerization of substances (lignin, cuticle, corky veins, etc.), and the complex structure formation of the anther cuticle[16,20]. Cytochrome P450 monooxygenase is a specific heme protein, an enzyme ubiquitous in various mammalian tissues, insects, plants, yeasts, and other species. It is mostly located in the endoplasmic reticulum of cells[21,22].

More than 670 CYPs have been named in plants and these genes play an important role in different stages of plant growth and development, especially the role of CYP86As is mainly related to fatty acid synthesis[13,23]. *GmCYP86A*s in soybean has been localized to fatty acid hydroxylase, which is involved in the biosynthesis of suberin monomer[24]. The expression of *CcCYP86A*s in capsicum were up-regulated in fruits with high cutin content[25]. Organ fusion occurs in rosette leaves and inflorescences of the *AtCYP86A8* mutant in *Arabidopsis*[23]. *AtCYP86A2* represses bacterial type III secretion system related

gene expression through the synthesis of cutin-associated fatty acids, thereby inhibiting pathogen infection[26]. Ectopic expression of *VvCYP86A1* in *Arabidopsis* showed a salt-tolerant phenotype[27]. *CsCYP86A*s in cucumber disrupt the cell membrane structure by increasing the level of free fatty acids to acclimatize the cucumber hypocotyl to water-soaked conditions[28]. However, how the CYP86As regulate cuticular wax accumulation has been less studied in apple.

Apple is one of the most important economic fruit trees in the world, and its quality affects the commodity value. Wax forms a film-like structure on the surface of apple fruit, which affects fruit gloss, reduces water loss to prolong shelf-time, reduces pest infection, and plays an important role in protecting the surface moisture and gloss of the fruit[3,29,30]. In this study, 28 genes of MdCYP86A in the apple genome were identified. MdCYP86As were analyzed by bioinformatics technology for physicochemical properties, phylogeny, gene structure, interspecies covariance, cis-acting elements, conserved motif, and domain. *MdCYP86A21* was identified in apple, which was highly expressed in flower. Subcellular localization showed that *MdCYP86A21* was localized in the endoplasmic reticulum, and improved drought and salt tolerance in apple calli. This provides a molecular basis for subsequent studies on the MdCYP86As involvement in wax accumulation in apple.

Methods

MdCYP86A family identification in apple

The family proteins were queried on the Pfam website (www.ebi.ac.uk/interpro). The HMM model of the family was obtained from HMMER software using the obtained ID number. The HMM model was compared to the apple genome using TBtools software to determine the final protein sequence. The members of this family were subsequently identified in TBtools software. The gene sequences of *Arabidopsis*, *Rice*, and *Tobacco* were downloaded from NCBI (www.ncbi.nlm.nih.gov) for subsequent analysis of CYP86As.

The MdCYP86As protein physicochemical properties analysis

The physicochemical properties of this family protein were predicted through the EXPASY online website (www.expasy.org), such as MW (KDa), isoelectric point (PI), number of amino acids, instability coefficient, and a series of other indicators.

Evolutionary tree, conserved motif, and domain analysis

Based on the previously obtained protein sequences of the family, the gene evolution tree of the family was drawn in MEGA11 software using the Neighbor-Joining (NJ) method. The protein sequences were uploaded to the MEME website (https://meme-suite.org/meme/tools/meme) to obtain the conserved motifs of this family during the evolutionary process. The predicted motifs were defaulted to 10, and the motif plots were further embellished through the Chiplot online website (www.chiplot.online/#Scatter-plot). The conserved structural domains of this family were queried using the CD-Search function in NCBI, and the graphs were subsequently embellished in the Chiplot website (www.chiplot.online/#Scatter-plot).

Gene structure and phylogenetic analysis

The protein sequences were uploaded to the GSDS online website (http://gsds.cbi.pku.edu.cn/), the gene structure of the family was mapped out, and the relevant values adjusted in the website to beautify the pictures. The homologous genes of the family in *Arabidopsis* (*Arabidopsis thaliana*), *Rice* (*Oryza sativa* L.), and *Tobacco* (*Nicotiana tabacum*) were blasted out using NCBI, and a multi-species phylogenetic tree was drawn in MEGA11 software.

Promoter analysis

Sequences of 2000 bp before the start codon of the family gene ATG were extracted from the Apple GDR online website (www.rosaceae.org). The sequence of the first 2,000 bp of ATG was uploaded to the PlantCARE website (https://bioinformatics.psb.ugent.be/webtools/plantcare/html/) to screen the cis-acting elements contained in the promoter sequences. It counts the number of elements using Excel, cis-acting elements visualization in TBtools, and the visualized images beautification by Adobe Illustrator 2022.

Chromosome location and covariance analysis

Screening the chromosome location of family genes and the length of the chromosome where they are located in the apple genome annotation file, using the MG2C website (http://mg2c.iask.in/mg2c_v2.1/index.html) for visualization, and adjusting the relevant parameters for beautification, a standard chromosome distribution map can be obtained. The apple genome files and annotation files were downloaded in NCBI, uploaded to TBtools, visualized in OneStepMCScanX plug-in, and the relevant parameters adjusted to beautify the covariance map.

Protein tertiary structure analysis and network analysis of interacting proteins

Protein sequences were uploaded to the Phyre2 website (www.sbg.bio.ic.ac.uk/phyre2/html/page.cgi?id=index) to predict the tertiary structure of proteins. Interacting protein network maps were drawn using the STRING website (https://cn.string-db.org/cgi/input?sessionId=b5yciQWPS93E&input_page_show_search=on).

RNA extraction and reverse transcription

RNA was extracted from GL3 wild-type apple seedlings using RNA extraction kit (Tiangen Bio, Beijing, China). GL3 wild-type apple seedlings needed to be treated under four conditions: normal growth, PEG, NaCl, and ABA. The samples were taken at 0, 1, 3, 6, 12, 24 and 48 h. The cDNA was synthesized by reverse transcription using the reverse transcription reagent (HiScript II Q Select RT SuperMix for qPCR, Vazyme). These were then analyzed by real-time fluorescence quantitative PCR (QuantStudio 7 Flex, Thermo Fisher, USA), using 18S as an internal reference gene.

Expression vector construction and Agrobacterium transformation

Design amplification primers were used to clone the full-length sequence of *MdCYP86A21* into PRI-101 vector to obtain overexpression plasmids. The sequence around 30 bp length in the full-length sequence was selected for reverse complementation, amplified, and cloned into the PRI-101 vector to obtain the suppression plasmid. The overexpression and suppression plasmid were transferred into Agrobacterium *LBA4404*. The primer sequences are shown in Supplemental Table S1.

Subcellular localization

The 35S::*MdCYP86A21*-RFP vector was constructed and transferred into Agrobacterium *LBA4404*, then transiently injected

into tobacco leaves. These were put under dark conditions for 1 d and put into the light. Subcellular localization pictures were taken on a laser confocal microscope LSM880 (Zeiss LSM 510 META, Jena, Germany) after 60 h.

Treatment of abiotic stress

The wild apple calli and transgenic calli were transferred to different medium treatments to observe the growth conditions. The wild apple calli, *MdCYP86A21*-OE and *antiMdCYP86A21*-PRI were five duplicate treatments. 4% PEG were used to simulate drought stress, 100 mM NaCl to simulate a salt environment. These were placed in resistance plates for 10–15 d in dark treatment to see the phenotypic changes and determine the relevant resistance index.

Determination of fresh weight and malondialdehyde.

Apple calli fresh weight using a 10,000 parts per million balance, and recording of data for follow-up statistics. MDA was determined using the Thiobarbituric acid method, referring to the methods of Wang et al.[31] 1 g of sample was ground on ice, 2 mL phosphate buffer and 5 mL thiobarbituric acid were then added. The solution was mixed well and put in boiling water for 10 min. After cooling, the absorbance values were measured at 450, 532, 600 nm using a UV spectrophotometer. The MDA content was calculated using the formula: MDA ($mmol \cdot g^{-1} \cdot FW$) = $[6.542 \times (OD_{532} - OD_{600}) - 0.559 \times OD_{450}] \times [V_t/(V_s \times FW)]$. V_t: total volume of extract. V_s: measured volume.

Data processing and statistical analysis

All data have more than three biological replicates. The error line indicates the standard deviation between samples. Lowercase letters indicate significant differences in samples at $p < 0.05$. Significance analyses were performed in SPSS.25, and plotting was performed in GraphPad Prism 8.0.

Results

Identification of MdCYP86A family genes in apple genome

Twenty-eight putative MdCYP86As, ranged from *MdCYP86A1* to *MdCYP86A28* were identified through analyzing and screening by HMMER software (Supplemental Table S2). The physicochemical properties of the MdCYP86As gene family were revealed. The physicochemical properties of the MdCYP86As family proteins were predicted using Expasy software. These result showed that the number of amino acids ranged from 423–753, the molecular weights ranged from 48.12–87.4 KDa, and the theoretical isoelectric points (PIs) ranged from 5.86–9.16. They were acidic proteins and their theoretical isoelectric points were less than 7, 23 proteins were alkaline proteins and their theoretical isoelectric points were greater than 7. Among all the proteins, the instability index of 12 proteins were less than 40 and 16 proteins were more than 40. It means that most of the MdCYP86As proteins are stable. The aliphatic index of all proteins were less than 100, and the total average hydrophobicity index was less than 0, which suggests that MdCYP86As proteins are hydrophilic proteins. The above analyses showed that most of the MdCYP86A family proteins were unstable hydrophilic alkaline protein (Table 1).

Localization distribution and the inter-species covariance of MdCYP86A family genes

Twenty-eight MdCYP86A genes chromosomes were found to be unevenly distributed on the 13 chromosomes of apple with

Table 1. The physicochemical properties of the MdCYP86As family proteins.

Sequence ID	Number of amino acids	Molecular weight	Theoretical pI	Instability index	Aliphatic index	Grand average of hydropathicity
MdCYP86A1	553	62,140.98	5.86	51.14	96.47	−0.029
MdCYP86A2	594	68,147.91	9.05	33.81	94.6	−0.183
MdCYP86A3	508	58,180.4	8.77	30.04	95.63	−0.131
MdCYP86A4	503	58,126.88	8.86	33.51	85.31	−0.213
MdCYP86A5	585	67,211.62	8.19	36.64	89.85	−0.221
MdCYP86A6	753	87,408.56	6.3	41.04	87.78	−0.232
MdCYP86A7	512	59,231.46	8.31	38.68	89.28	−0.138
MdCYP86A8	522	58,977.08	9.16	41.38	90.65	−0.161
MdCYP86A9	524	59,217.2	8.85	39.72	90.5	−0.124
MdCYP86A10	508	57,785.03	8.2	40.48	84.45	−0.306
MdCYP86A11	535	60,662.44	8.15	43.34	94.64	−0.081
MdCYP86A12	513	58,460.27	8.84	40.19	94.56	−0.066
MdCYP86A13	516	59,081.04	7.97	42.69	89.59	−0.178
MdCYP86A14	525	59,381.74	6.17	50.18	97.89	−0.042
MdCYP86A15	423	48,120.41	6.35	35.13	92.25	−0.194
MdCYP86A16	514	58,923.46	7.95	44.63	89.32	−0.131
MdCYP86A17	506	57,795.41	8.9	41.48	86.5	−0.234
MdCYP86A18	506	57,541.1	9.03	41.64	85.18	−0.236
MdCYP86A19	522	59,333.65	8.59	30.91	94.16	−0.104
MdCYP86A20	544	62,600.47	8.45	37.62	88.88	−0.176
MdCYP86A21	574	65,958.23	8.81	39.96	89.51	−0.229
MdCYP86A22	521	59,981.17	8.65	38.03	94.45	0.034
MdCYP86A23	534	60,600.33	8.68	40.6	95.51	−0.098
MdCYP86A24	512	58,494.1	9.02	41.24	92.48	−0.088
MdCYP86A25	520	59,435.27	8.3	41.37	88.71	−0.192
MdCYP86A26	523	60,084.98	6.38	46.06	92.1	−0.152
MdCYP86A27	507	58,722.86	8.55	35.93	91.68	−0.113
MdCYP86A28	506	57,839.15	7.55	47.57	89.98	−0.092

some distributional preferences. Chromosome 2 contained the largest quantities of MdCYP86A family members. *MdCYP86A4*, *MdCYP86A5*, *MdCYP86A6*, and *MdCYP86A7* were closely arranged on the chromosomes, which suggests that they may have undergone tandem duplication events during the long period of gene amplification and evolution (Fig. 1a & Supplemental Table S3). The gene amplification enhanced their expression level, improved the function of genes, and facilitated the evolution and adaptation of organisms. These results suggested that gene duplication event displays function in the amplification and evolution of the MdCYP86A family.

An interspecies covariance analysis between the CYP86A family genes in *Apple* and the homologous genes in *Arabidopsis*, *Rice*, and *Tobacco*, respectively. We found that the gene duplication frequency between *Apple* and *Arabidopsis* was the highest, with 31 covariances. This was followed by *Rice* with nine covariates. These indicated that the CYP86A family genes in *Apple* and *Arabidopsis* have the highest homology and the two species are most closely related to each other (Fig. 1b).

Phylogenetic and gene structure of MdCYP86As

To realize the evolutionary relationship of CYP86As in multi-species, CYP86As from *Apple*, *Arabidopsis thaliana*, *Rice*, and *Tobacco* were jointly constructed into a phylogenetic evolutionary tree. They were divided into three branches I, II, and III (Supplemental Table S4). Among which 18 MdCYP86As proteins belonged to the I branch and 10 MdCYP86As proteins belonged to the II branch. The similar gene structure between gene family members suggests that they may have similar transcriptional regulatory and splicing machines, which in turn led to the understanding of gene family regulation and expression patterns (Fig. 2a). In the gene structure analysis of 28 MdCYP86A proteins showed that each protein sequence contained exons, numbering from 1–9. Among them, *MdCYP86A2* has the maximum number of exons. These exons were longer than the introns and distributed at both ends of the sequence. MdCYP86As exons and introns have similar distribution patterns, which shows members are closely evolutionarily related and have similar expression patterns (Fig. 2b).

Evolutionary and conserved motif analysis of MdCYP86A gene in apple

To study the evolutionary relationships of MdCYP86A genes, the evolutionary tree of the family was drawn using MEGA11, and found that 28 family genes were closely related to each other. In addition, most of the evolutionary distances greater

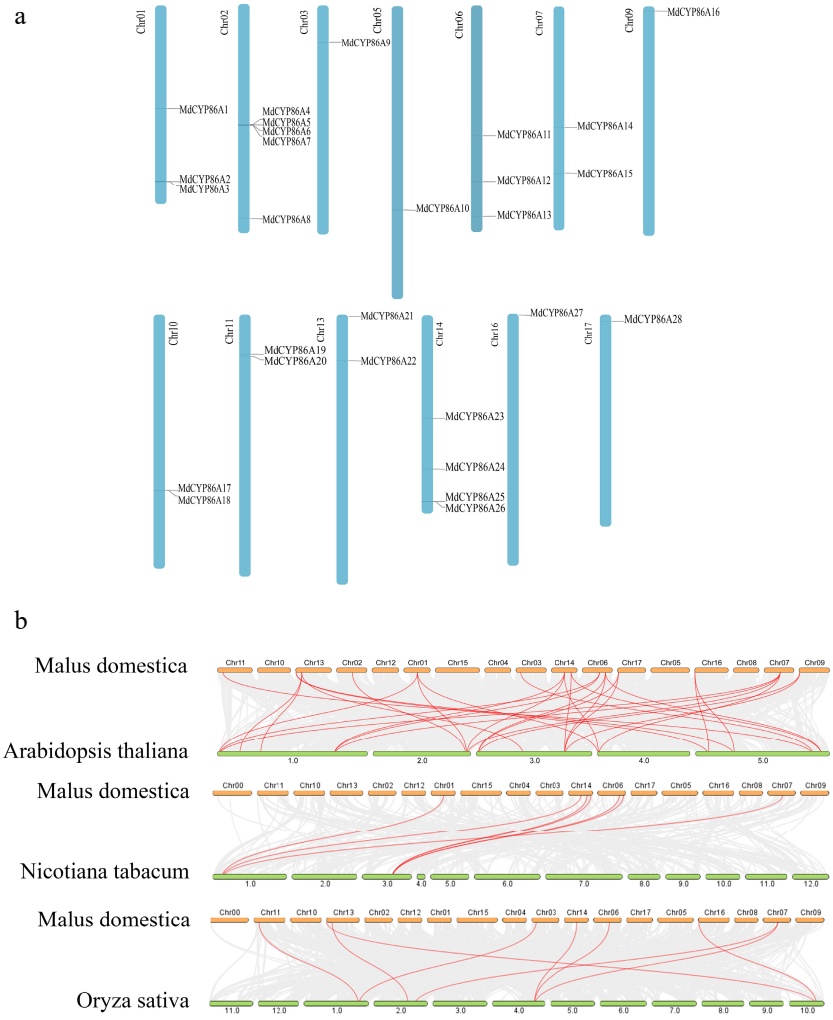

Fig. 1 Localization distribution and the inter-species covariance of MdCYP86A family genes. (a) Distribution of MdCYP86A family genes on 13 apple chromosomes. (b) Analysis of covariance in *Apple*, *Arabidopsis*, *Tobacco*, *Rice*.

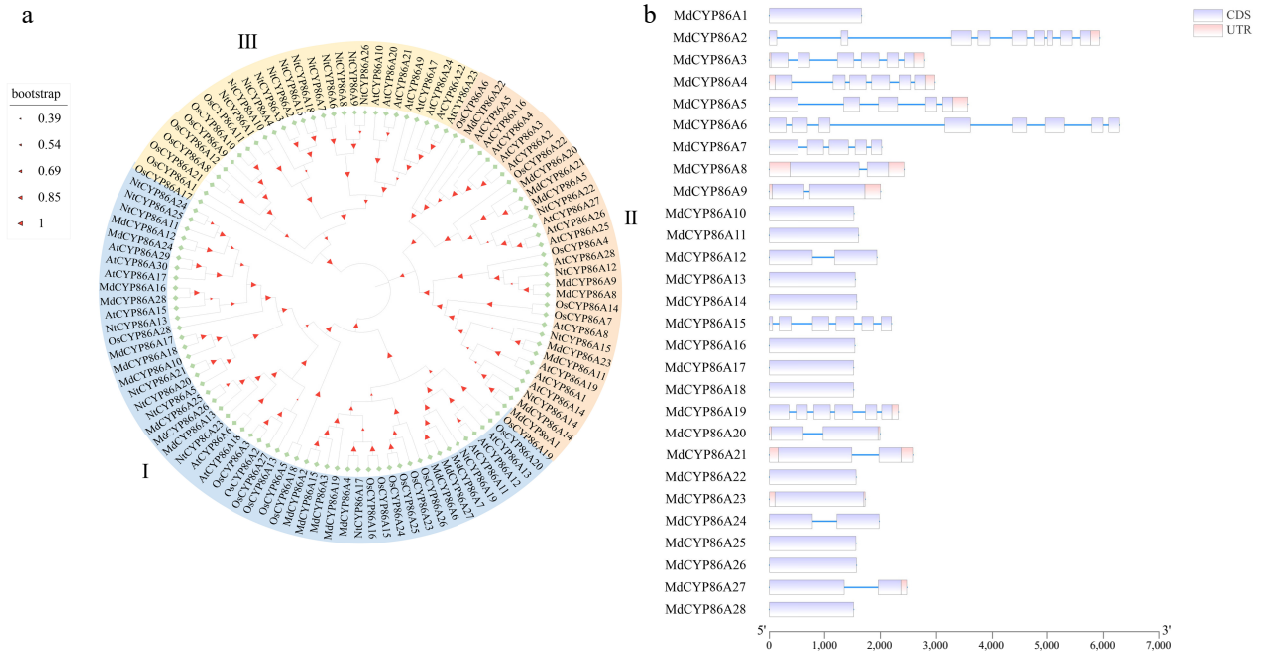

Fig. 2 Phylogenetic and gene structure of MdCYP86As. (a) Phylogenetic tree construction in MEGA software for CYP86A family genes in four species: *Arabidopsis thaliana*, *Rice*, *Tobacco,* and *Apple*. (b) Gene structure analysis of MdCYP86A subfamily genes in apple, including both CDS and UTR regions.

than 80, which indicated that the family was highly conserved (Fig. 3a). Based on the family evolutionary tree, the MEME website was used to analyze the conserved motifs, and more than 10 motifs were screened (Fig. 3b). Although the number of motifs in each sequence varied, each gene possessed more than eight motifs, and the distribution of motifs in the sequences was generally consistent, indicating that these 10 motifs were highly conserved in this family (Supplemental Fig. S1). The conserved structural domains of MdCYP86As were also batch screend in NCBI, and found that all 28 protein sequences contained CYP86A structural domains, which all contained specific binding sites (Fig. 3c). However, *MdCYP86A6* contains not only the CYP86A structural domain but also the cytochrome P450 subfamily structural domain, which contains a non-specific binding site. It was speculated that this gene is likely to bind some specific endogenous and exogenous redox compounds of the substrate, thus catalyzing the redox reaction of the substrate (Fig 3c). Because *MdCYP86A21* has the greatest variety of stress-related response elements, including ARE, STRE, LTR, MRE and so on. The protein 3D structure of *MdCYP86A21* was predicted. It showed that the MdCYP86As family proteins have high similarity in 3D structure (Fig. 3d & Supplemental Fig. S2).

Cis-acting element analysis

Upstream cis-acting elements of promoters are important for the selection of gene transcription start sites and transcription rates. By analyzing the types and numbers of cis-acting elements upstream in promoters, the regulatory mechanisms of gene family members can be revealed, which leads to a deeper understanding of the functions and roles of the family members. To identify 28 conserved cis-acting elements within the promoter region of the MdCYP86As, the 2,000 bp sequences upstream of the ATG start codon were submitted to the PlantCARE database for promoter prediction analysis. These cis-acting elements were classified into four categories, including growth-associated, light-associated, stress-associated and hormone-associated. Among the growth and development-related cis-acting elements, the main elements are involved in endosperm expression (AAGAA-motif), shoot expression (As-1), correlation with meristematic tissue expression (CAT-box), endosperm-specific expression element (GCN4-motif), and senescence expression (W-box), which are contained in the first 2,000 bp upstream of most the MdCYP86A gene promoter cis-acting elements with bud expression (As-1) and had the highest proportion (34%) with the number of 41. In the light response element category, TCCC-motif had the largest proportion. In the stress response-related category, they were associated with anaerobic induction (ARE, GC-motif) and resist stress (STRE, TC-rich repeats), trauma (WRE3, WUN-motif), metal-response (MRE), cold-response (LTR) and drought-response (MBS), with the highest number of defense stress (STRE). And in the hormone response element category included abscisic acid (ABRE, ABRE3a, ABRE4), growth hormone (TGA-element), gibberellin (P-box, TATC-box), jasmone acid (CGTCA-motif, TGACG-motif, MYB, MYC), salicylic acid (TCA), and ethylene-responsive (ERE) response elements, with the largest proportion of cis-acting elements responding to jasmone acid (MeJA). Since hormone-signaling substances have more important roles in plants with biotic and abiotic stresses, the elements involved in the stress response and hormone response may be involved in the regulation of expression in apple interaction with adversity. Because hormonal signaling closely related with responding to stress, hormone-related elements in MdCYP86As promoter suggests that this family of genes may be involved in the regulation of expression in apple and adversity interactions (Fig. 4). These showed that the promoters of the MdCYP86As contain a variety of response elements that can be recognized and bound by different transcription factors involved in plant growth, development, and stress response.

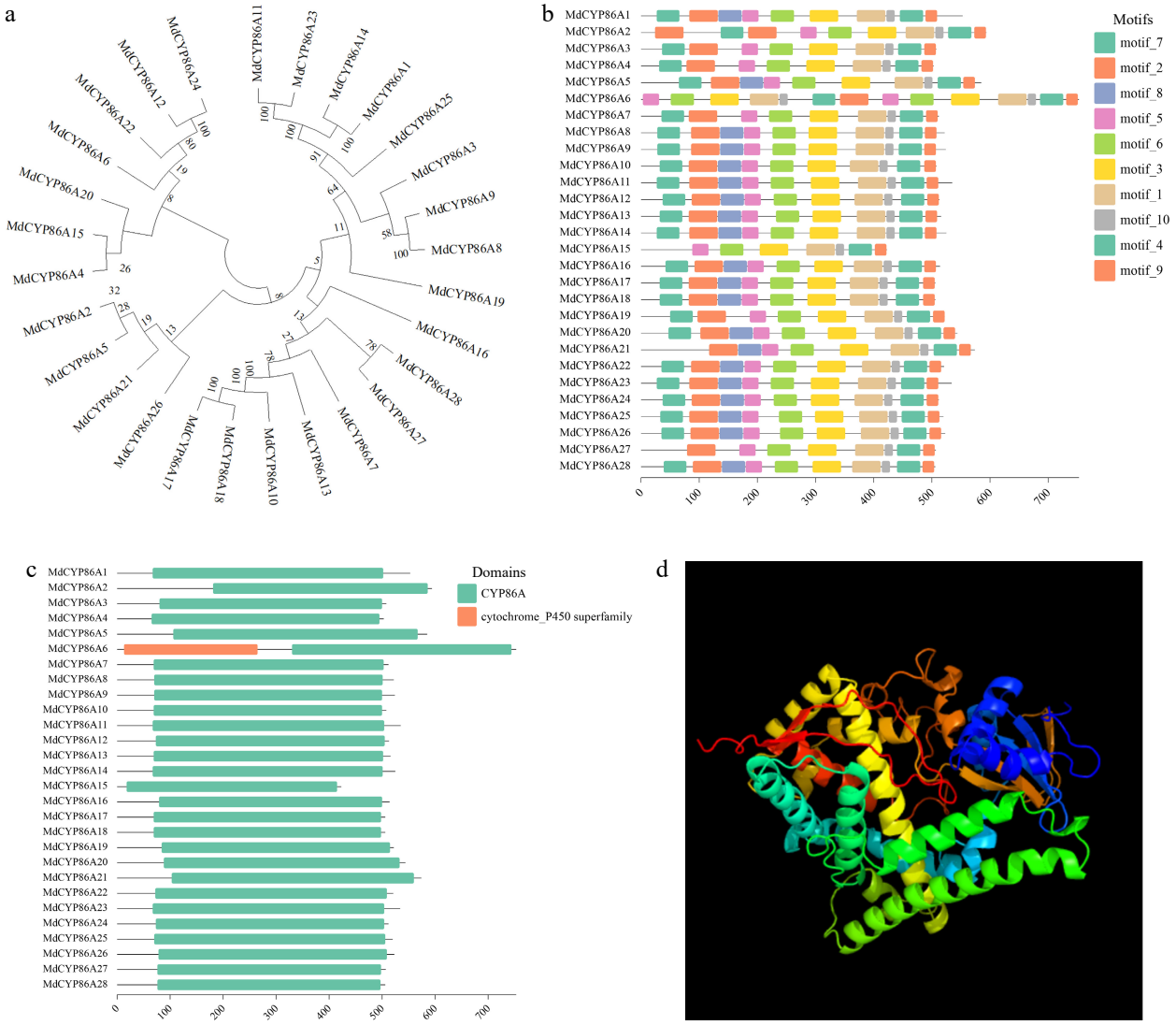

Fig. 3 Evolutionary and conserved motif analysis of MdCYP86As gene in apple. (a) Construction of MdCYP86A subfamily evolutionary tree in MEGA11 software, the numbers next to the branches represent the evolutionary proximity between genes. (b) MdCYP86A subfamily motif analysis, on the left side is the gene ID of the family, and different colored boxes represent different motifs, with sequence length scale bar underneath. (c) The MdCYP86A subfamily conserved structural domains are analyzed, with gene ID on the left, structural domain on the right, and sequence length scale bar below. (d) Protein 3D structure image of *MdCYP86A21*.

Expression patterns of *MdCYP86A21* in different tissues and abiotic stress

Previous analyses of cis-acting elements showed that the MdCYP86A family genes all contain different numbers of promoter elements under abiotic stress, we examined whether *MdCYP86A21* is differentially expressed under PEG, NaCl, and ABA abiotic stresses. Compared to the control, NaCl treatment resulted in the highest expression at 3 h, followed by a decrease reaching a minimum at 12 h, and then increasing again at 24 h. The expression of PEG treatment was lower than the control in the early stage. Until 24 h, the expression reached about eight times the control, then decreased. The expression was elevated at 3 h, and then peaked at 12 h, which was about 27 times of the control, and then decreased to about six times of the control in ABA treatment. The above results suggest that *MdCYP86A21* has a relative function in the response to abiotic stresses (Fig. 5a).

Tissue-specific expression patterns revealed that *MdCYP86A21* was mainly expressed in flowers, followed in by root and fruit, with the lowest expression in leaves, *MdCYP86A21* function primarily in flowers (Fig. 5b). 35S::*MdCYP86A21*-RFP was constructed using the full sequence of *MdCYP86A21*. RFP empty vector was also injected into tobacco. The empty vector was observed to fluoresce in both the nucleus and the cell membrane under laser confocal microscopy. 35S::*MdCYP86A21*-RFP appeared net structure and overlapped with the endoplasmic reticulum marker (PAL2259). From the results, it could be determined that *MdCYP86A21* is a membrane protein which localizes endoplasmic reticulum (Fig. 6).

MdCYP86A21 improves the tolerance to PEG and NaCl

To further investigate the role of *MdCYP86A21* to abiotic stresses in apple, overexpressed (*MdCYP86A21*-OE) was obtained and suppressed (*antiMdCYP86A21*-PRI) transgenic calli

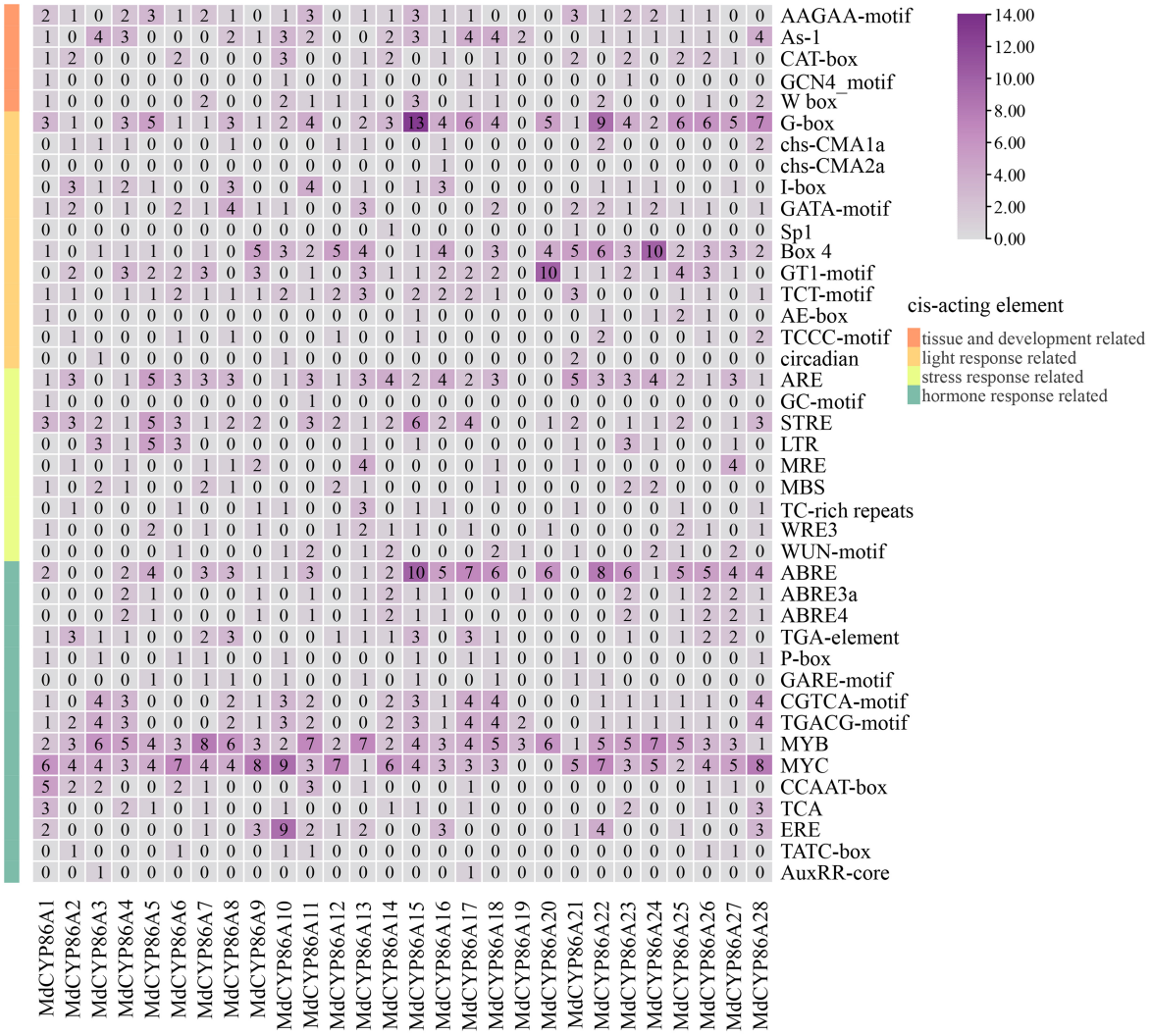

Fig. 4 Cis-acting elements analysis of the MdCYP86A subfamily. The classification of the different types of elements on the left, the gene ID below, and the name of the element on the right. The number representing the number of elements, and a larger number representing higher numbers of that element.

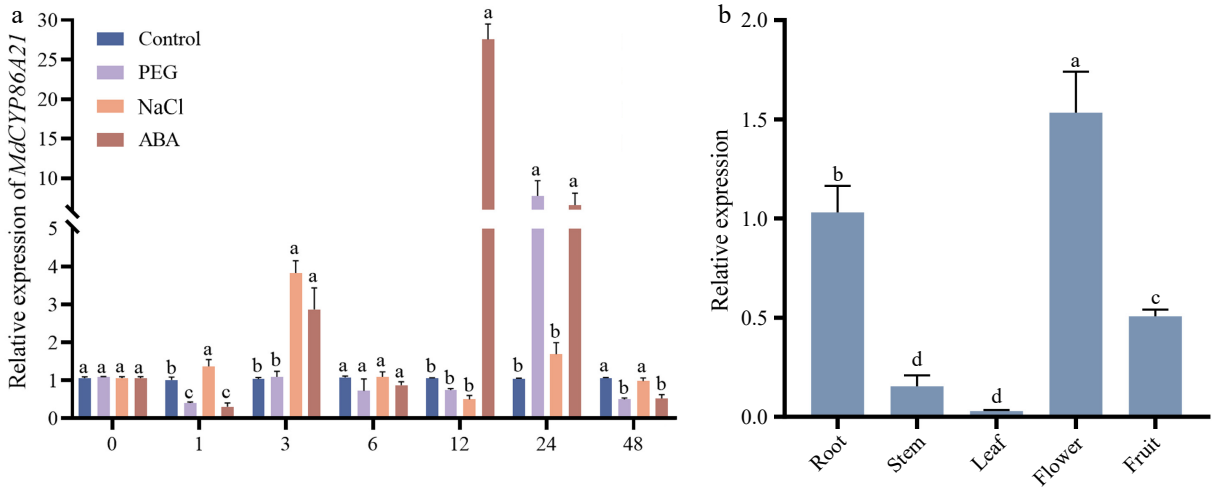

Fig. 5 Expression patterns of *MdCYP86A21* in different tissues and abiotic stress. (a) Expression pattern of *MdCYP86A21* in response to three abiotic stresses, including PEG, NaCl and ABA. There are three biological replicates of the data, $p < 0.05$. (b) Expression levels of *MdCYP86A21* in root, stem, leave, flower and fruit, there are three biological replicates of the data, $p < 0.05$.

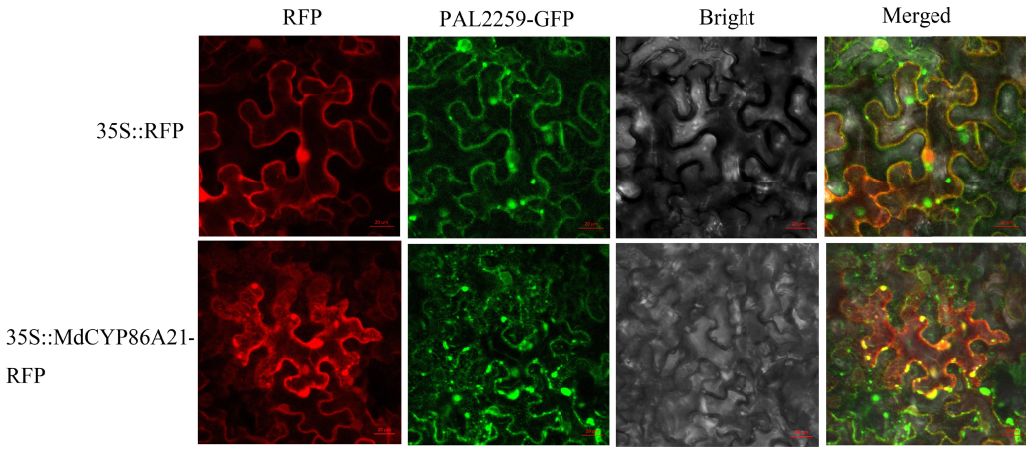

Fig. 6 Subcellular localization of *MdCYP86A21*, scale bar = 20 μm.

were obtained to detect the resistance of abiotic stresses (Supplemental Fig. S3). The results showed that there was no significant difference in the fresh weight of WT, *MdCYP86A21*-OE, and *antiMdCYP86A21*-PRI in MS. But in MS with 4% PEG and 100 mM NaCl, the fresh weight of *MdCYP86A21*-OE was significantly increased and *antiMdCYP86A21*-PRI was significantly decreased compared to the wild type (Fig. 7a & b). The content of MDA was significantly decreased in *MdCYP86A21*-OE than wild type. *MdCYP86A21* improves apple calli resistance to PEG and NaCl (Fig. 7c). These results suggested that *MdCYP86A21* responded to PEG and NaCl stresses, and improved drought and salt resistance.

MdCYP86A21 interacting protein prediction

In order to further investigate the molecular mechanism of *MdCYP86A21* involved in wax biosynthesis, *MdCYP86A21* interacting proteins were predicted. In the predicted network, almost all proteins are related to fatty acid biosynthesis. Among them, *ACOT* is an acyl-coA thiesterase, which is involved in the hydrolysis of fatty acyl CoA. *FAD* is a fatty acid dehydrogenase involved in the synthesis of wax esters to promote oleaginous greasiness. *CER2* and *CYP86A7* are directly involved in wax biosynthesis (Fig. 8).

Discussion

Cytochrome P450 is one of the largest protein families in plants[32]. CYP86As participated in the synthetic processes of fatty acids and alkanes[33]. Current research on CYP86As is mainly in the biosynthesis of suberin monomers, disease resistance, and response to abiotic stresses. *PpyCYP86B1* in pear is transcriptionally activated by *PpyMYB114* to regulate suberin monomer accumulation in the pericarp[34]. *GhCYP86A1-1* in cotton functions in resisting Xanthomonas campestris[35]. *AtCYP86A1* in Arabidopsis is involved in suberin monomer biosynthesis[36]. *SlCYP86As* in tomato is involved in the synthesis of cork lipids and improves drought tolerance in tomato seedlings[37]. In this study, MdCYP86As were studied with regard to the abiotic stress in apple. The 28 members of MdCYP86A were identified in the apple genome, *MdCYP86A21* was cloned to validate its resistant function in drought and salt, laying a foundation for future research on the impact of abiotic stress through wax synthesis.

Gene duplication events are crucial in the process of gene evolution, since species can genetically expand family genes and acquire new genes and the new genes' emergence enhances the adaptation of species to the environment and promotes the evolution of species[38]. Tandem duplication events occur in both the chromosomal localization and cis-acting element results for MdCYP86As (Figs 1a & 4). A large number of duplications of sequences such as SINE and L1 in mammals lead to changes in the timing and level of expression of developmental genes, and duplications of the L1 element led to the specific activation or silencing of genes with different functions at a specific time[39]. Following the results of covariance suggests that the tandem duplication events promote gene family hybridization and species evolution. However, the covariance in *Tobacco* and *Rice* was significantly less than *Arabidopsis* (Fig. 1b). This suggests that the functional expression of CYP86As in *Rice* and *Tobacco* declined with evolution. The gene structure, motif, and domain of MdCYP86As were highly similar, suggesting that CYP86As evolved in a relatively conserved evolutionary manner in apple (Figs 2b & 3). However, two conserved structural domains are present in *MdCYP86A6* and it is speculated that this gene has a stronger ability to select response substrates (Fig. 3c).

The P450 family is a monooxygenase, the site where it binds substrates and functions is mainly the endoplasmic reticulum[13,26]. Consistent with the results of previous studies, *MdCYP86A21* was mainly expressed in flower (Fig. 5b). This is consistent with the results of the *MdCYP86A21* subcellular localization (Fig. 6). In the wax biosynthesis pathway, C16 and C18 fatty acids were intended to very long chain fatty acid (VLCFA). They were further extended into C20–C34 fatty acids in endoplasmic reticulum. Afterward, the alkane, alcohol, aldehyde, ketone, and ester are produced by various enzymes in the endoplasmic reticulum. Wax biosynthesis was almost exclusively carried out in subcellular organelles, after which wax monomers were transported to the plasma membrane and cuticle *via* transporter proteins[14,40,41]. *MdCYP86A21* was located in the endoplasmic reticulum. It was speculated that *MdCYP86A21* may be involved in the wax biosynthesis process.

Previous studies have shown that members of the CYP86A family involved in plant response and regulation to adversity. For example, under salt stress, the expression of the *CYP86A2* gene is significantly up-regulated, which promotes the

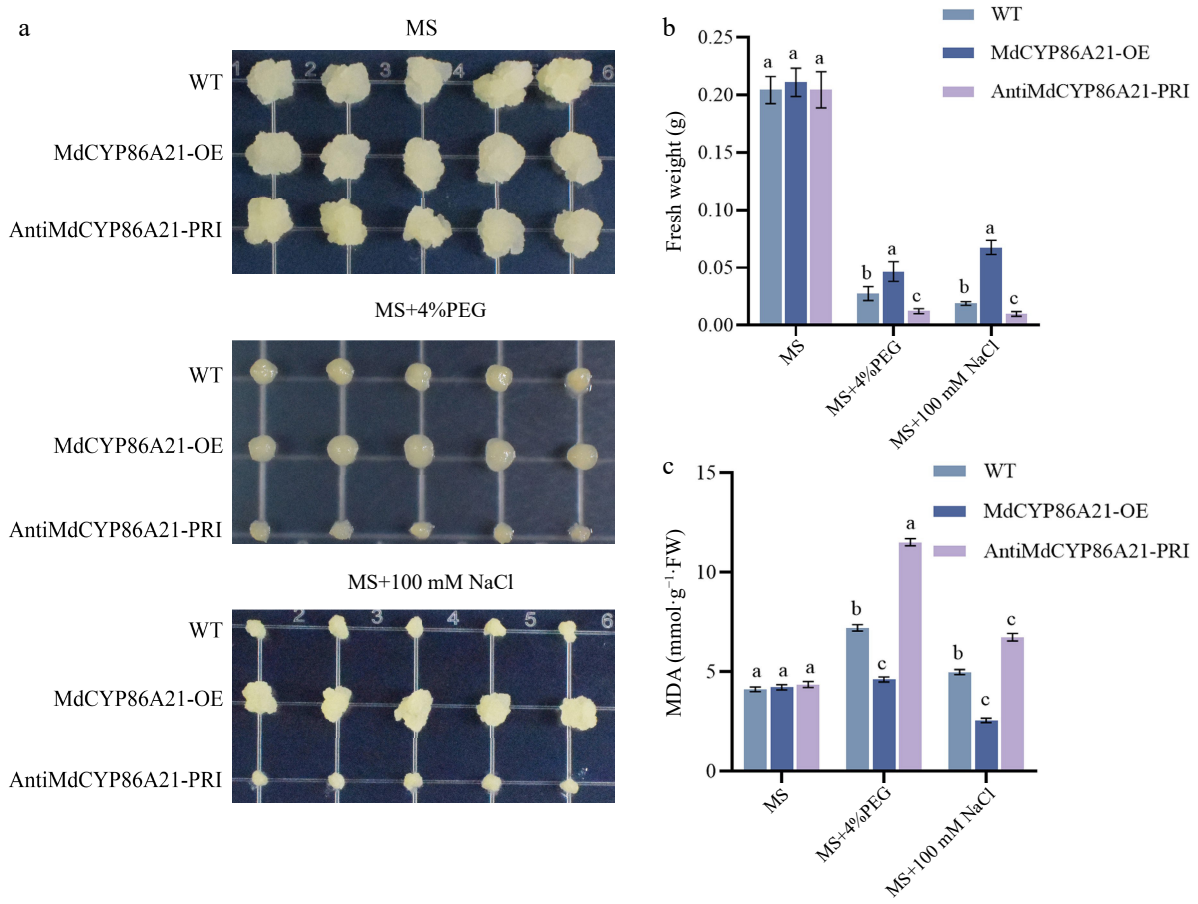

Fig. 7 *MdCYP86A21* improves the tolerance to PEG and NaCl. (a) *MdCYP86A21* apple calli treated on MS, PEG, NaCl medium for 15 d, the first row is wild type, the second is overexpression, and the third is suppression, five replicates per treatment. (b) Fresh weight of wild-type, overexpressed, and suppression calli were determined under different treatments. (c) Determination of MDA content in wild-type, overexpressed, and suppression calli under different treatments.

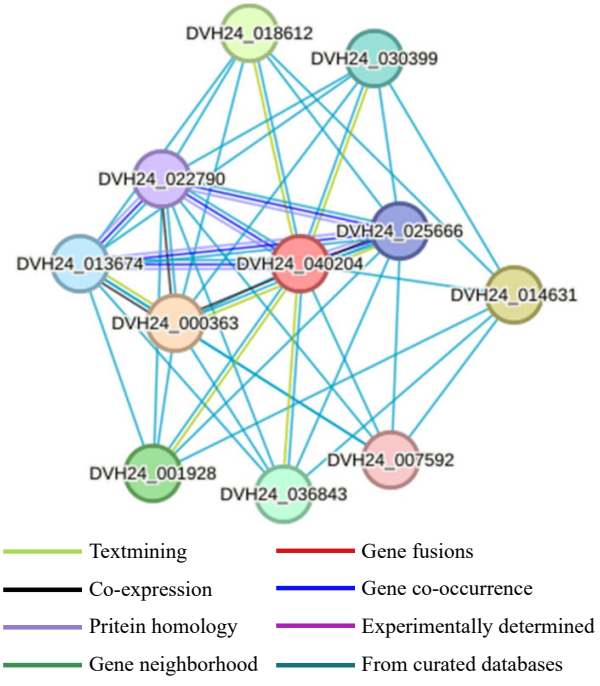

Fig. 8 Protein interactions network analysis of *MdCYP86A21*.

synthesis of hydroxy fatty acids, improves the stability and tolerance of cell membranes, and enhances the ability to adapt to salt stress[42]. *MdCYP86A21* contains components of the corresponding stresses (Fig. 4). qRT-PCR showed that *MdCYP86A21* was corresponded to PEG and NaCl (Fig. 5a). Meanwhile, *MdCYP86A21* showed tolerance in drought and salt in apple calli (Fig. 7). These results suggested that MdCYP86As are involved in responding to abiotic stresses. The predicted proteins are almost all related to fatty acid synthesis, such as *ACOT*, *CER2*, *FAD*, *CYP86A7*[43–47]. This provides a molecular basis for the subsequent validation of the *MdCYP86A21* function (Fig. 8).

Finally, there are a variety of enzymes involved in wax biosynthesis, and research on wax synthesis pathways will continue. In this study, MdCYP86As were identified from the apple genome and carried out bioinformatics analysis. MdCYP86As is the closest relationship with *Arabidopsis*. This family is highly conservative in apple evolution. The gene structure, conserved motif, and domain are extremely similar in MdCYP86As protein sequences. *MdCYP86A21* was cloned and its function preliminarily verified in apple abiotic stress. *MdCYP86A21* showed tolerance in drought and salt in apple calli. This provides a basis for the subsequent validation of *MdCYP86A21* in apple fruits. This will provide a candidate gene for the subsequent development of stress tolerance in apple and improvement of fruit quality.

Author contributions

The authors confirm contribution to the paper as follows: study conception and design: Li YY, Zhang YL; performing the experiments, data analysis, interpretation of results, and draft manuscript preparation: Lv HM; assisting in experiments: Qi RH, Yu ZH, Man YY, Jiang H, Lv YH, Wang T. All authors reviewed the results and approved the final version of the manuscript.

Data Availability

The datasets generated during and/or analyzed during the current study are available from the corresponding author on reasonable request.

Acknowledgments

This work was supported by the National Key R&D Plan Project (2023YFD2301000), National Natural Science Foundation of China (32072539), Natural Science Foundation of Shandong Province (ZR2022JQ14), and Taishan Scholar Project.

Conflict of interest

The authors declare that they have no conflict of interest.

Supplementary Information accompanies this paper at (https://www.maxapress.com/article/doi/10.48130/frures-0024-0024)

Dates

Received 9 May 2024; Revised 28 June 2024; Accepted 2 July 2024; Published online 2 September 2024

References

1. Zhang Y, Zhang C, Wang G, Wang Y, Qi C, et al. 2019. The R2R3 MYB transcription factor MdMYB30 modulates plant resistance against pathogens by regulating cuticular wax biosynthesis. *BMC Plant Biology* 19:362
2. Yeats TH, Rose JKC. 2013. The formation and function of plant cuticles. *Plant Physiology* 163:5–20
3. Zhang Y, Tian Y, Man Y, Zhang C, Wang Y, et al. 2023. Apple SUMO E3 ligase MdSIZ1 regulates cuticular wax biosynthesis by SUMOylating transcription factor MdMYB30. *Plant Physiology* 191:1771–88
4. Wang H, Lu Z, Xu Y, Zhang J, Han L, et al. 2023. Roles of very long-chain fatty acids in compound leaf patterning in *Medicago truncatula*. *Plant Physiology* 191:1751–70
5. Huang H, Yang X, Zheng M, Chen Z, Yang Z, et al. 2023. An ancestral role for 3-KETOACYL-COA SYNTHASE3 as a negative regulator of plant cuticular wax synthesis. *The Plant Cell* 35:2251–70
6. Kong L, Liu Y, Zhi P, Wang X, Xu B, et al. 2020. Origins and evolution of cuticle biosynthetic machinery in land plants. *Plant Physiology* 184:1998–2010
7. Kunst L, Samuels L. 2009. Plant cuticles shine: advances in wax biosynthesis and export. *Current Opinion in Plant Biology* 12:721–27
8. Wu Y, Lv Y, Li X, Gao H, Zhou M, et al. 2024. The effect of epigallocatechin-3-gallate (EGCG), a main active ingredient in tea residues, on improving fruit quality and prolonging postharvest storage in apple. *Scientia Horticulturae* 326:112782
9. Lian X, Gao H, Jiang H, Liu C, Li Y. 2021. MdKCS2 increased plant drought resistance by regulating wax biosynthesis. *Plant Cell Reports* 40:2357–68
10. Declercq M, Alkio M, Sprink T, Schreiber L, Knoche M. 2014. Effect of sweet cherry genes *PaLACS2* and *PaATT1* on cuticle deposition, composition and permeability in *Arabidopsis*. *Tree Genetics & Genomes* 10:1711–21
11. Li J, Zhang C, Zhang Y, Gao H, Wang H, et al. 2022. An apple long-chain acyl-CoA synthase, *MdLACS1*, enhances biotic and abiotic stress resistance in plants. *Plant Physiology and Biochemistry* 189:115–25
12. Man Y, Lv Y, Lv H, Jiang H, Wang T, et al. 2024. *MdDEWAX* decreases plant drought resistance by regulating wax biosynthesis. *Plant Physiology and Biochemistry* 206:108288
13. Kandel S, Sauveplane V, Olry A, Diss L, Benveniste I, et al. 2006. Cytochrome P450-dependent fatty acid hydroxylases in plants. *Phytochemistry Reviews* 5:359–72
14. Greer S, Wen M, Bird D, Wu X, Samuels L, et al. 2007. The cytochrome P450 enzyme CYP96A15 is the midchain alkane hydroxylase responsible for formation of secondary alcohols and ketones in stem cuticular wax of Arabidopsis. *Plant Physiology* 145:653–67
15. Zhou M, Yu Z, Gao H, Li M, Wu Y, et al. 2023. Ectopic expression of an apple ABCG transporter gene *MdABCG25* increases plant cuticle wax accumulation and abiotic stress tolerance. *Fruit Research* 3:43
16. Nelson D, Werck-Reichhart D. 2011. A P450-centric view of plant evolution. *The Plant Journal* 66:194–211
17. Bak S, Beisson F, Bishop G, Hamberger B, Höfer R, et al. 2011. Cytochromes P450. *The Arabidopsis Book* 9:e0144
18. Sun C, Liu Y, Li G, Chen Y, Li M, et al. 2024. *ZmCYP90D1* regulates maize internode development by modulating brassinosteroid-mediated cell division and growth. *The Crop Journal* 12:58–67
19. Li L, Chang Z, Pan Z, Fu Z, Wang X. 2008. Modes of heme binding and substrate access for cytochrome P450 CYP74A revealed by crystal structures of allene oxide synthase. *Proceedings of the National Academy of Sciences of the United States of America* 105:13883–88
20. Tanaka Y, Brugliera F. 2013. Flower colour and cytochromes P450. *Philosophical Transactions of the Royal Society B: Biological Sciences* 368:20120432
21. Nelson DR, Schuler MA. 2013. Cytochrome P450 genes from the sacred lotus genome. *Tropical Plant Biology* 6:138–51
22. Bozak KR, Christoffersen RE. 1992. Expression of a ripening-related avocado (*Persea americana*) cytochrome P450 in Yeast. *Plant Physiology* 100:1976–81
23. Pinot F, Beisson F. 2010. Cytochrome P450 metabolizing fatty acids in plants: characterization and physiological roles. *The FEBS Journal* 278:195–205
24. Tully TLA, Kaushik P, O'Connor J, Bernards MA. 2020. Fatty acid ω-hydroxylases of soybean: *CYP86A* gene expression and aliphatic suberin deposition. *Botany* 98:317–26
25. Natarajan P, Akinmoju TA, Nimmakayala P, Lopez-Ortiz C, Garcia-Lozano M, et al. 2020. Integrated metabolomic and transcriptomic analysis to characterize cutin biosynthesis between low- and high-cutin genotypes of *Capsicum chinense* Jacq. *International Journal of Molecular Sciences* 21:1397
26. Xiao F, Mark Goodwin S, Xiao Y, Sun Z, Baker D, et al. 2004. *Arabidopsis CYP86A2* represses Pseudomonas syringae type III genes and is required for cuticle development. *The EMBO Journal* 23:2903–13
27. Xuenan Zhang, Yao Ge, Xue Yang, Yan Ma, Lingmin Dai, et al. 2021. Overexpression of Vvcyp86a1 Improves salt tolerance in *Arabidopsis thaliana* during germination and seedling stages. *Chemistry and Medical Engineering* 2021:109–117
28. Xu X, Chen M, Ji J, Xu Q, Qi X, et al. 2017. Comparative RNA-seq based transcriptome profiling of waterlogging response in cucumber hypocotyls reveals novel insights into the de novo adventitious root primordia initiation. *BMC Plant Biology* 17:129

29. Gao L, Cao J, Gong S, Hao N, Du Y, et al. 2023. The COPII subunit *CsSEC23* mediates fruit glossiness in cucumber. *The Plant Journal* 116:524–40
30. Zhang C, Hu X, Zhang Y, Liu Y, Wang G, et al. 2020. An apple *long-chain acyl-CoA synthetase 2* gene enhances plant resistance to abiotic stress by regulating the accumulation of cuticular wax. *Tree Physiology* 40:1450–65
31. Wang X, Yang F, Zhang J, Ren Y, An J, et al. 2023. Ectopic expression of *MmCYP1A1*, a mouse cytochrome P450 gene, positively regulates stress tolerance in apple calli and *Arabidopsis*. *Plant Cell Reports* 42:433–48
32. Werck-Reichhart D, Feyereisen R. 2000. Cytochromes P450: a success story. *Genome Biology* 1:reviews3003.1
33. Hansen CC, Nelson DR, Møller BL, Werck-Reichhart D. 2021. Plant cytochrome P450 plasticity and evolution. *Molecular Plant* 14:1244–65
34. Zhang J, Liu Z, Zhang Y, Zhang C, Li X, et al. 2023. *PpyMYB144* transcriptionally regulates pear fruit skin russeting by activating the cytochrome P450 gene *PpyCYP86B1*. *Planta* 257:69
35. Wang G, Xu J, Li L, Guo Z, Si Q, et al. 2020. *GbCYP86A1-1* from *Gossypium barbadense* positively regulates defence against *Verticillium dahliae* by cell wall modification and activation of immune pathways. *Plant Biotechnology Journal* 18:222–38
36. Höfer R, Briesen I, Beck M, Pinot F, Schreiber L, et al. 2008. The *Arabidopsis* cytochrome P450 *CYP86A1* encodes a fatty acid ω-hydroxylase involved in suberin monomer biosynthesis. *Journal of Experimental Botany* 59:2347–60
37. He Y. 2012. *Structural polymers and molecular pathways that influence tomato fruit integrity and surface quality traits*. Thesis. Cornell University, NY.
38. Flagel LE, Wendel JF. 2009. Gene duplication and evolutionary novelty in plants. *New Phytologist* 183:557–64
39. Richardson SR, Doucet AJ, Kopera HC, Moldovan JB, Garcia-Perez JL, et al. 2015. The influence of LINE-1 and SINE retrotransposons on mammalian genomes. *Microbiology Spectrum* 3:MDNA3-0061-2014
40. Nelson DR. 2011. Progress in tracing the evolutionary paths of cytochrome P450. *Biochimica et Biophysica Acta (BBA) - Proteins and Proteomics* 1814:14–18
41. Zhang C, Wang Y, Hu X, Zhang Y, Wang G, et al. 2020. An apple AP2/EREBP-type transcription factor, *MdWRI4*, enhances plant resistance to abiotic stress by increasing cuticular wax load. *Environmental and Experimental Botany* 180:104206
42. Sun K, Fang H, Chen Y, Zhuang Z, Chen Q, et al. 2021. Genome-wide analysis of the cytochrome P450 gene family involved in salt tolerance in *Gossypium hirsutum*. *Frontiers in Plant Science* 12:685054
43. Wen H, Wang Y, Wu B, Feng Y, Dang Y, et al. 2021. Analysis of wheat wax regulation mechanism by liposome and transcriptome. *Frontiers in Genetics* 12:757920
44. Zhao Y, Peng T, Sun H, Teotia S, Wen H, et al. 2019. miR1432-*OsACOT* (Acyl-CoA thioesterase) module determines grain yield via enhancing grain filling rate in rice. *Plant Biotechnology Journal* 17:712–23
45. Yang X, Wu D, Shi J, He Y, Pinot F, et al. 2014. Rice CYP703A3, a cytochrome P450 hydroxylase, is essential for development of anther cuticle and pollen exine. *Journal of Integrative Plant Biology* 56:979–94
46. Zhong M, Jiang H, Cao Y, Wang Y, You C, et al. 2020. *MdCER2* conferred to wax accumulation and increased drought tolerance in plants. *Plant Physiology and Biochemistry* 149:277–85
47. Jiang Z, Ding Y, Liu J, Yin W, Qi Y, et al. 2022. The *MdFAD27* and *MdFAD28* play critical roles in the development of greasiness disorder in postharvest apples. *Postharvest Biology and Technology* 191:111990